Macromolecules

pubs.acs.org/Macromolecules Article

One-Step Synthesis of Statistical Copolymers Containing Peptide, Ester, Ether, and Amine Linkages via *N*-Substituted Glycine *N*-Carboxyanhydrides and Epoxides

Keke Zhang, Weier Wu, Tianlun Shen, Peng Zhou, Tianwen Bai, and Jun Ling*

Cite This: *Macromolecules* 2025, 58, 9450−9458 Read Online

ACCESS | Metrics & More | Article Recommendations | Supporting Information

ABSTRACT: The ring-opening copolymerization of α-amino acid *N*-carboxyanhydrides (NCA) with nitrogen-free monomers including cyclic esters and epoxides recently emerged as a fascinating method to synthesize α-amino acid-based copolymers with backbones containing not only peptide linkages but also ester and ether ones. It enriched the toolbox for the modulation of the properties of polypeptides and polypeptoids as biomaterials and thermoplastic elastomers. Whereas, balancing the activities of nitrogen- and oxygen-terminal living centers in a single catalytic system was extremely challenging. In this contribution, the first example of random copolymerization of *N*-substituted glycine NCAs with epoxides was succeeded catalyzed by transition-metal triflates including lutetium triflate ($Lu(OTf)_3$). The copolymers with four types of linkages including amide, ether, ester, and tertiary amine groups were synthesized in a one-step and one-pot procedure. The molar ratios of cyclohexene oxide (CHO) to sarcosine NCA (Sar-NCA) in copolymers were designed from 0.17:1 to 0.51:1 and the $M_{n,SEC}$ of P(Sar-*co*-CHO) varied between 2.4 and 27.0 kg/mol. The copolymerization followed a coordination anionic ring-opening mechanism and was versatile for various alkyl- and aryl-substituted glycine NCAs as well as diverse epoxides such as CHO, propyl oxide (PO), and 1,2-epoxy-4-vinylcyclohexane (VCHO). P(Sar-*co*-CHO) was noncytotoxic and biodegradable by porcine pancreatic lipase due to the ester linkages in its backbone. P(Sar-*co*-VCHO), a PSar with multiple vinyl pendant groups, was capable of forming a hydrogel through thio-ene click reaction. In summary, we provided a novel, simple, and efficient approach to synthesize random copolymers of *N*-substituted glycine NCAs with epoxides, thereby diversifying the copolymer structures and advancing the synthetic methodology for the copolymerization of NCA with nitrogen-free monomers.

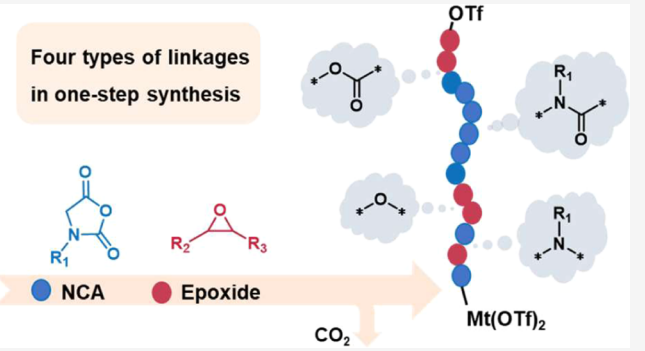

INTRODUCTION

Polypeptoids, as structural isomers of natural polypeptides, garnered significant attention in biomedical fields over the past decades due to their good solubility, excellent biocompatibility, and easy modification.[1−3] Ring-opening polymerizations (ROPs) of *N*-substituted glycine *N*-carboxyanhydrides (NCAs) and *N*-thiocarboxyanhydrides (NTAs) were powerful methods widely used to synthesize polypeptoids with high molecular weights, narrow distributions, and precise sequence control.[1,4−6] In order to meet diverse demands in drug delivery[7,8] and nonfouling surfaces,[9,10] the properties of polypeptoids were modulated through the copolymerization of different NCAs or NTAs.[11] Whereas, the approach focused primarily on modifying side chains, while the backbone remained rigid and linked exclusively by amide groups, thus limiting the extent of property modulation.

Recent interest was aroused in the copolymerization of α-amino acid NCA or NTA with nitrogen-free monomers, such as cyclic esters and epoxides.[3,12−15] The approach enriched the variety of backbone structures in copolymers, which led to tunable properties suitable for biomaterials and thermoplastic elastomers.[16−21] However, it presented significant challenges under a single catalytic system to balance the reactivity of the nitrogen-terminal growing centers after the addition of NCA or NTA with the oxygen-terminal growing centers from cyclic esters and epoxides. In 2023, Byers et al. reported a redox-switchable polymerization of sarcosine NCA (Sar-NCA) and cyclohexene oxide (CHO) to prepare block copolymers catalyzed by an iron complex.[13] However, the reactions of NCA and CHO were orthogonal, i.e., NCA polymerized only under the reduced state of the iron complex while CHO only under the oxidized one. Recently, Wang's group developed a Lewis pair-catalyzed chemo-selective polymerization method

Received: June 10, 2025
Revised: August 15, 2025
Accepted: August 19, 2025
Published: August 26, 2025

https://doi.org/10.1021/acs.macromol.5c01539
Macromolecules 2025, 58, 9450−9458

Scheme 1. Copolymerization of NCAs with Epoxides

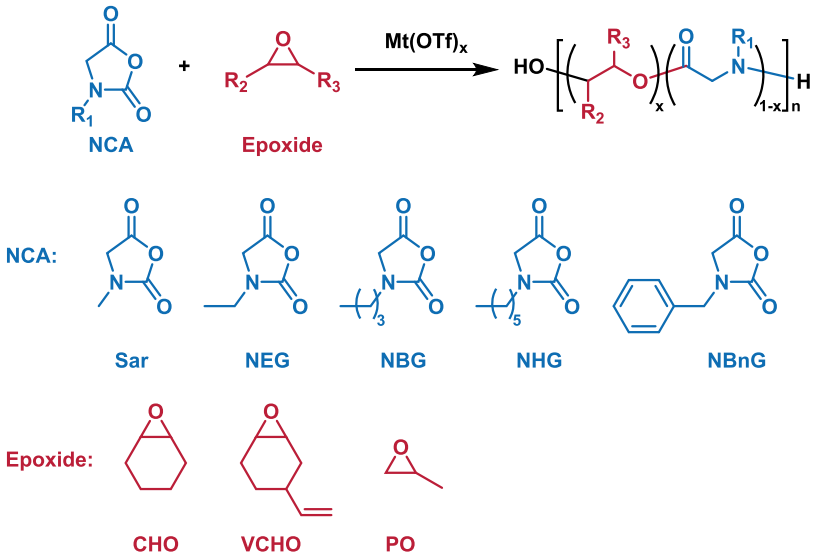

Table 1. Copolymerization of NCAs with Epoxides Catalyzed by $Lu(OTf)_3$

run[a]	AA-NCA[b]	epoxide	solvent[c]	time (days)	cat.:NCA:epoxide in feed	conv. of NCA (%)[d]	conv. of epoxide (%)[e]	epoxide:AA in polymer[f]	$M_{n,theo}$ (kg/mol)[g]	$M_{n,SEC}$ (kg/mol)[h]	$Đ$[h]
1	Sar	CHO	ACN	2	1:100:200	>99	19	0.37:1	10.7	11.5	1.64
2	Sar	CHO	DMF	2	1:100:200	>99	8	0.15:1	8.6	7.5	1.44
3	Sar	CHO	DMAc	2	1:100:200	>99	8	0.15:1	8.6	7.8	1.31
4	Sar	CHO	DCM	2	1:100:200	24	9	0.71:1	3.4	6.0	1.28
5	Sar	CHO	DCE	2	1:100:200	25	9	0.69:1	3.5	6.1	1.32
6	Sar	CHO	ACN	4	1:30:100	>99	14	0.46:1	3.5	2.4	1.17
7	Sar	CHO	ACN	2	1:60:120	>99	21	0.42:1	6.7	10.7	1.61
8	Sar	CHO	ACN	2	1:200:400	>99	9	0.18:1	17.7	16.7	1.62
9	Sar	CHO	ACN	2	1:400:800	>99	5	0.10:1	32.3	27.0	1.43
10	Sar	CHO	ACN	2	1:100:50	>99	34	0.17:1	8.8	11.5	1.56
11	Sar	CHO	ACN	2	1:100:100	>99	27	0.27:1	9.8	12.9	1.65
12	Sar	CHO	ACN	2	1:100:400	>99	13	0.51:1	12.1	8.9	1.77
13	Sar	VCHO	ACN	2	1:100:200	>99	5	0.09:1	8.2	12.7	1.68
14	Sar	VCHO	ACN	2	1:100:400	>99	4	0.17:1	9.2	9.0	1.65
15	Sar	PO	ACN	2	1:30:60	>99	15	0.29:1	2.7	2.7	1.13
16	Sar	PO	ACN	2	1:100:200	>99	6	0.12:1	7.8	4.4	1.09
17	Sar	PO	ACN	2	1:200:400	>99	4	0.07:1	15.0	5.2	1.09
18	NEG	CHO	MTHF	3	1:65:65	95	23	0.24:1	7.1	4.5	1.32
19	NBG	CHO	ACN	4	1:65:65	>99	30	0.30:1	9.3	3.1	1.42
20	NHG	CHO	ACN	2	1:30:60	>99	23	0.45:1	5.6	1.6[i]	1.14[i]
21	NBnG	CHO	ACN	2	1:30:90	>99	42	1.26:1	8.2	1.5[i]	1.20[i]
22	NEG	CHO	ACN	2	1:100:200	95	10	0.20:1	10.0	13.3	1.37
23	NBG	CHO	ACN	2	1:100:200	96	13	0.27:1	13.4	9.6	1.55
24	NHG	CHO	ACN	2	1:100:200	97	8	0.17:1	15.3	2.0[i]	1.73[i]
25	NBnG	CHO	ACN	2	1:100:200	[j]	[j]				

[a]Polymerization conditions: initial concentration $[NCA]_0$ = 1 mol/L at 60 °C. [b]α-Amino acid NCA. [c]Acetonitrile (ACN), *N*,*N*-dimethylformamide (DMF), *N*,*N*-dimethylacetamide (DMAc), dichloromethane (DCM), 1,2-dichloroethane (DCE), 2-methyl-tetrahydrofuran (MTHF). [d]Determined by ^{1}H NMR. [e]Calculated from conversion (NCA) × feed ratio (NCA/epoxide) × content ratio (epoxide/AA in polymer) × 100%. [f]Ratio of epoxide and α-amino acid (AA) calculated from ^{1}H NMR of purified product. [g]Calculated from M(AA) × NCA:Cat. in feed × conv. of NCA + M(epoxide) × epoxide:Cat. in feed × conv. of epoxide + 18. [h]Determined by SEC in HFIP. [i]Determined by SEC in THF. [j]Formation of precipitates during copolymerization.

successfully producing poly(peptide-*b*-ester) from monomer mixtures of NCA and L-lactide in one step.[12] It revealed a huge reactivity difference between NCA and L-lactide catalyzed by the Lewis pair. In the copolymerization, homopolymerization of NCAs was completed within 1 h, followed by an approximately 2 h dormant period. The living polypeptide blocks were then reactivated for the polymerization of L-lactide. These results highlighted the challenges in achieving random copolymerization of NCAs or NTAs with nitrogen-free monomers.

In this contribution, we reported the random copolymerization of *N*-substituted glycine NCA with epoxide for the first

https://doi.org/10.1021/acs.macromol.5c01539
Macromolecules 2025, 58, 9450−9458

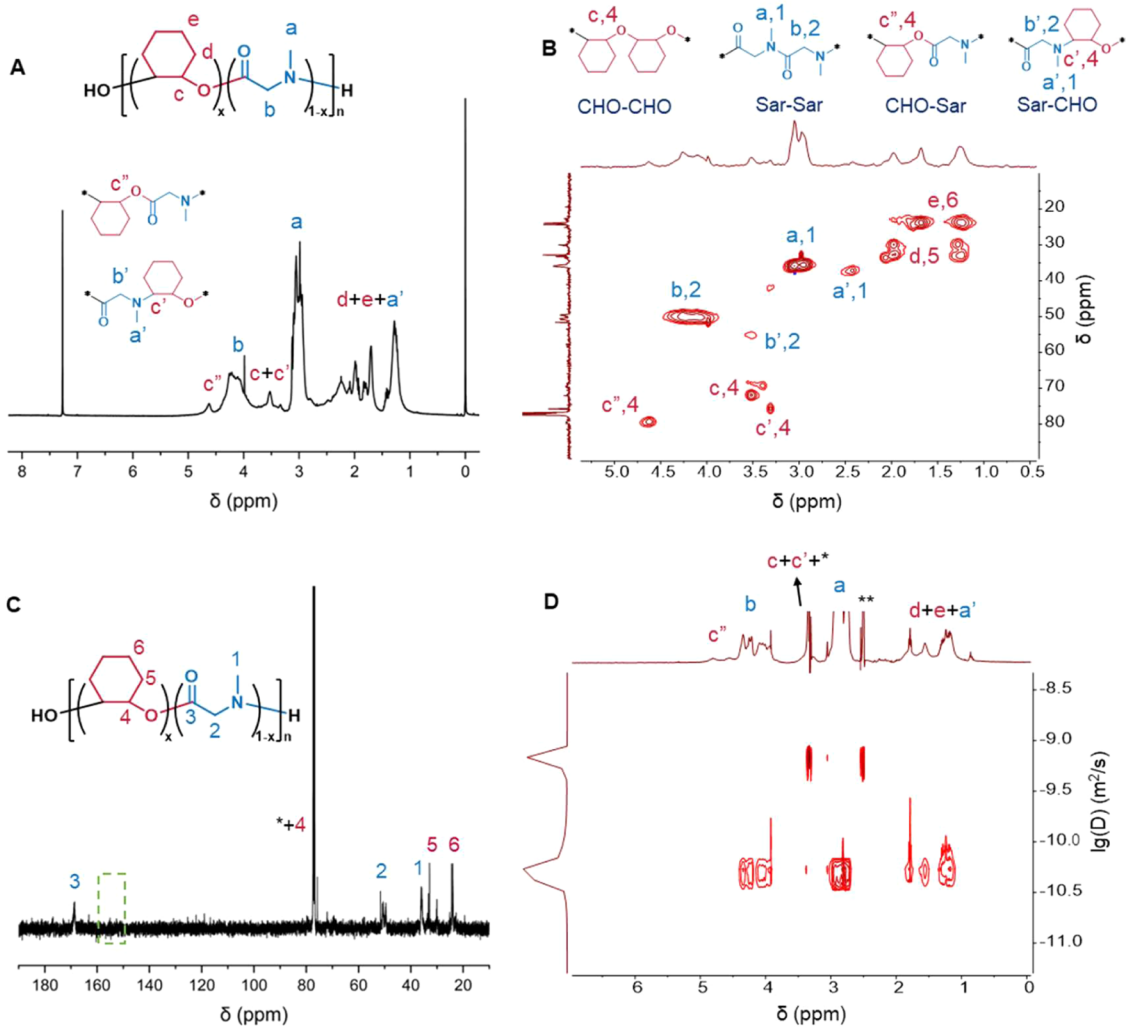

Figure 1. ^{1}H NMR (A), HSQC NMR (B), and ^{13}C NMR (C) spectra of P(Sar-*co*-CHO) in $CDCl_3$ (run 6 in Table 1, * $CHCl_3$) and DOSY NMR (D) spectrum of P(Sar-*co*-CHO) in DMSO-d_6 (run 1 in Table 1, * H_2O, ** DMSO).

time. The backbone of the copolymers of *N*-substituted glycine NCAs with epoxides consisted of four types of linkages, including amide, ester, ether, and tertiary amine groups, which facilitated diverse and tunable properties for application. Since the copolymers were mainly composed of *N*-substituted glycine residues as well as ester linkages, they retained the properties of polypeptoids and became biodegradable by lipase, resulting in biodegradable polypeptoids. The number-average molecular weight ($M_{n,SEC}$) of copolymers of sarcosine and CHO decreased by 65% after an incubation with porcine pancreatic lipase for 36 h.

Transition-metal triflate salts such as lutetium triflate ($Lu(OTf)_3$) and iron triflate ($Fe(OTf)_3$) were employed as the catalysts, which showed the advantages of commercial availability, low cost, and nontoxicity. The copolymerization proceeded via coordination anionic ring-opening polymerization (AROP), which was uncommon for metal triflates widely regarded as Lewis acids. The copolymerization method was versatile for *N*-substituted glycine NCAs bearing a variety of alkyl and aryl side groups, as well as different epoxides like CHO, propyl oxide (PO), and 1,2-epoxy-4-vinylcyclohexane (VCHO). P(Sar-*co*-CHO) was amphiphilic and formed spherical nanoparticles in water, demonstrating potential for application in drug delivery. Functionalized PSar containing double bonds was efficiently prepared through the copolymerization of Sar-NCA with VCHO capable of forming hydrogel via thio-ene click reaction with D,L-dithiothreitol.

RESULTS AND DISCUSSION

All of the *N*-substituted glycine NCAs were synthesized according to previous reports[22,23] and characterized by nuclear magnetic resonance (NMR) analyses (Figures S1−S9). Copolymerization of Sar-NCA with CHO was carried out at 60 °C and catalyzed by lutetium(III) triflate ($Lu(OTf)_3$) (Scheme 1). The polymerization rate of Sar-NCA was faster in polar solvents than in nonpolar ones. Sar-NCA was fully converted in *N*,*N*-dimethylformamide (DMF), *N*,*N*-dimethylacetamide (DMAc), and acetonitrile (ACN) within 2 days, whereas its conversion did not reach 30% in dichloromethane (DCM) and 1,2-dichloroethane (DCE) (runs 1−5 in Table 1). Among the polar solvents, the copolymers showed the highest CHO content in ACN under the same initial feed ratio, and thus ACN was the optimal solvent for the copolymerizations. The $M_{n,SEC}$ of copolymers were tunable from 2.4 to 27.0 kg/mol by increasing the feed ratio of monomers to catalyst (runs 1 and 6−9 in Table 1). The molar ratios of CHO units to Sar residues in copolymers were controlled between 0.17:1 and 0.51:1 in accordance with the increasing feed ratio of CHO to

https://doi.org/10.1021/acs.macromol.5c01539
Macromolecules 2025, 58, 9450−9458

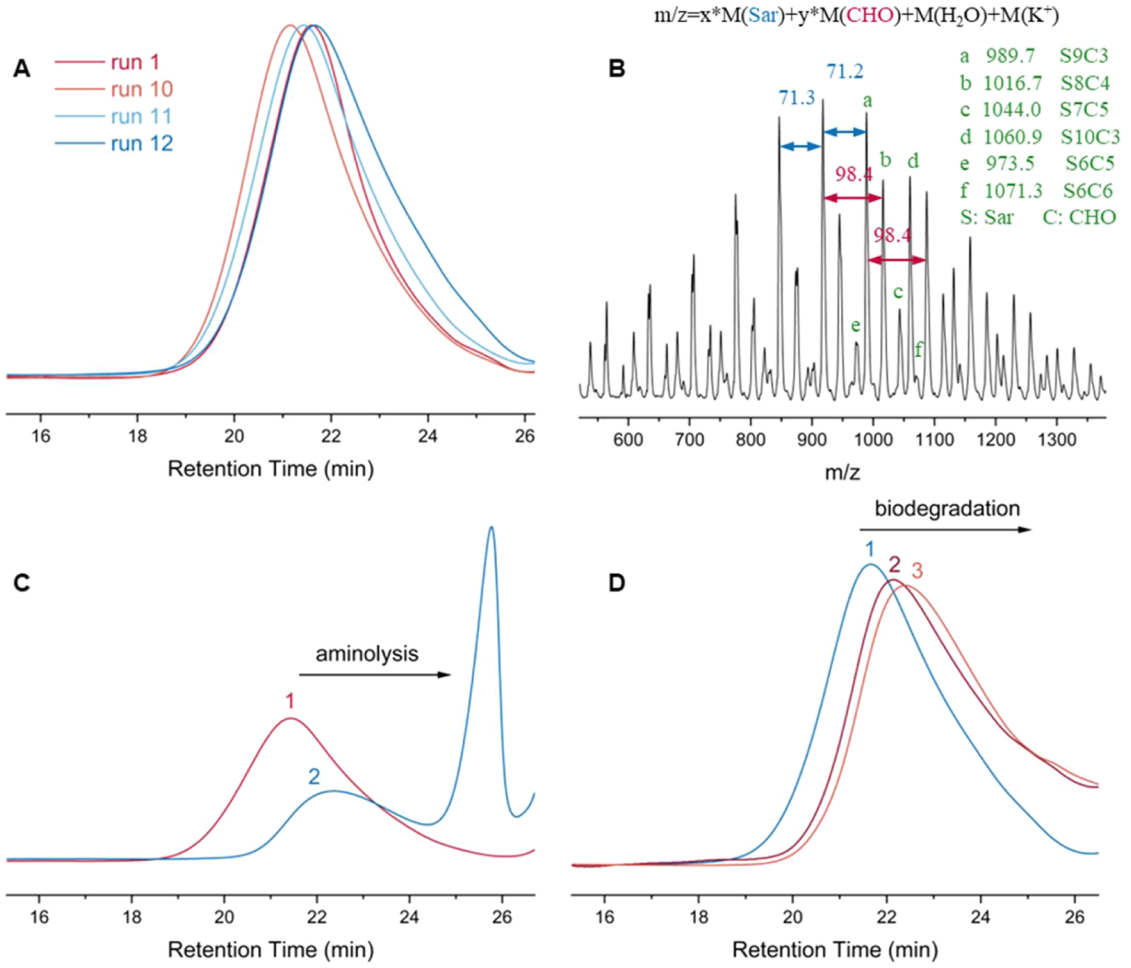

Figure 2. (A) SEC traces of P(Sar-*co*-CHO) in HFIP (runs 1, 10−12 in Table 1). (B) MALDI-ToF mass spectrum of P(Sar-*co*-CHO) (run 6 in Table 1). (C) SEC traces in HFIP of P(Sar-*co*-CHO) (run 6 in Table 1, red line 1) and the product after aminolysis (blue line 2). (D) SEC traces in HFIP of P(Sar-*co*-CHO) (blue line 1) (run 12 in Table 1) and the product after biodegradation by porcine pancreatic lipase (incubation for 36 h, red line 2; incubation for 7 days, orange line 3).

Sar-NCA (runs 1 and 10−12 in Table 1). The reproducibility of the copolymerization was verified under the typical conditions (1([Lu]):100(NCA):200(CHO) in ACN; Table S1), as demonstrated by the consistent comonomer incorporation ratios, $M_{n,SEC}$, and dispersities ($Đ$) across independently prepared batches under identical conditions.

The chemical structure of P(Sar-*co*-CHO) was fully characterized (Figures 1, 2A,B, and S10). The ^{1}H NMR spectra of the copolymers displayed typical proton signals of Sar residues at 2.85−3.10 ppm (H_a) and 3.84−4.48 ppm (H_b), and those of CHO units at 1.06−2.65 ppm ($H_{d\text{-}e}$), 3.28−3.75 ppm (H_c and $H_{c'}$), and 4.64 ppm ($H_{c''}$) with various diad linkages (Figure 1A). In the ^{13}C NMR spectra, the signals attributed to Sar residues (C_{1-3}) and CHO units (C_{4-6}) were also identified (Figure 1C). No signal was observed between 150 and 160 ppm, indicating that there was not any carbonate or carbamate group in the copolymers and that carbon dioxide (CO_2) was completely eliminated after Sar-NCA insertion and did not react with CHO during copolymerization.[24] CHO-Sar, Sar-CHO, and CHO−CHO diads were identified in a heteronuclear single quantum coherence (HSQC) NMR spectrum (Figure 1B). The correlation signal $H_{c''}$-C_4 (4.64, 79.6 ppm) was attributed to the methine next to the ester group from the CHO-Sar diads, while the signal H_c-C_4 (3.52, 72.1 ppm) was attributed to the methine linked to the ether bond from the CHO−CHO diads. Sar-CHO diads were confirmed by the correlation signals of $H_{a'}$-C_1 (2.44, 37.4 ppm) ascribed to *N*-methyl, $H_{b'}$-C_2 (3.54, 55.3 ppm) to *N*-methylene, and $H_{c'}$-C_4 (3.33, 75.7 ppm) to *O*-methine. The extensive signals of both CHO-Sar and Sar-CHO diads observed in the copolymers were solid evidence for random copolymers of P(Sar-*co*-CHO). In the diffusion-ordered spectroscopy (DOSY) NMR spectrum, all proton signals of the product exhibited an identical diffusion coefficient (Figure 1D), whereas those of the PSar and PCHO blends with comparable $M_{n,SEC}$ values displayed distinct values (Figure S11). This result confirmed the growth of sarcosine residues and CHO units within one single polymer chain rather than a blend of two types of homopolymers. Additionally, the size exclusion chromatography (SEC) traces of the copolymers showed a unimodal distribution, which further supported a uniform propagating species and consistent reactivity (Figure 2A). Both mass intervals of Sar residues (71 Da) and CHO units (98 Da) were observed in the matrix-assisted laser desorption/ionization time-of-flight (MALDI-ToF) mass spectrum of the products. The absolute mass of each population with K^+ cationization was consistent with the

https://doi.org/10.1021/acs.macromol.5c01539
Macromolecules 2025, 58, 9450−9458

Scheme 2. Coordination AROP Mechanism of Copolymerization of Sar-NCA with CHO

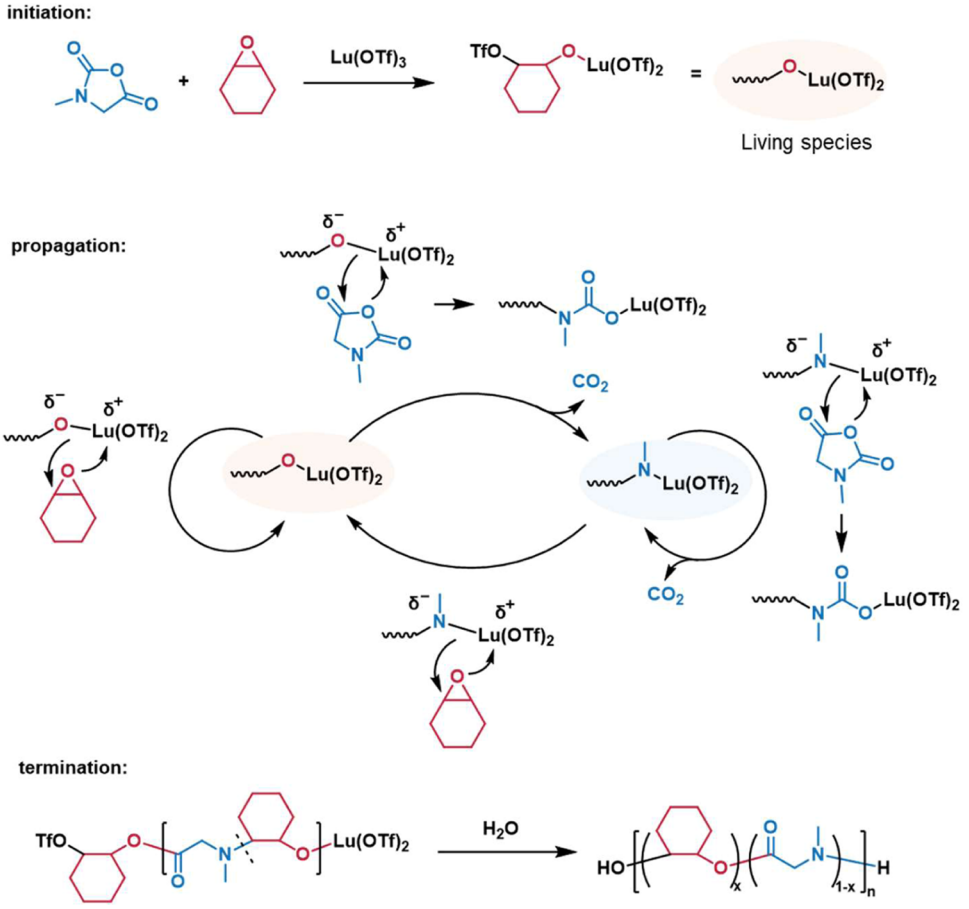

corresponding composition of random copolymers terminated by water (Figure 2B).

Owing to the presence of the ester bond from CHO-Sar diads in P(Sar-*co*-CHO) backbone, the copolymers were able to be aminolyzed by neopentylamine (Figure S12).[25] The proton signal of ester groups ($H_{c''}$, 4.64 ppm) disappeared after aminolysis, indicating their cleavage to become the *N*-neopentyl amide (Figure S13). The degradation of P(Sar-*co*-CHO) was evidenced by the decrease of $M_{n,SEC}$ of the copolymers from 11.5 to 1.8 kg/mol (Figure 2C). The aminolyzed product was separated into two parts after precipitation in ether (Table S2). The precipitate consisted of polymers mainly composed of Sar residues with an average degree of polymerization (DP) of 26 according to the signal intensities of *N*-neopentyl amide protons at the polymer chain end (Figures S14 and S15), indicating the presence of homo-PSar segments not degradable in P(Sar-*co*-CHO) copolymers. The supernatant contained soluble oligomers of PSar-*b*-PCHO, PSar, and PCHO, which were confirmed by ^{1}H NMR and high-resolution quadrupole time-of-flight mass spectrometry (HRMS) (Figure S16). The two blocks of PSar-*b*-PCHO were linked via tertiary amine from Sar-CHO diads of the original copolymers, validating the NMR analysis results.

The kinetic study provided more detailed insights into the copolymerization process. $M_{n,SEC}$ of the copolymers increased as the reaction time was prolonged (Figure S17). After a 9 h induction period, Sar-NCA was consumed following first-order kinetics (k_p = 0.22 h^{-1}). The conversion of CHO did not reach 50% even if the reaction time was prolonged to 40 h (Figures S18 and S19). The reactivity ratios of two monomers were (r(Sar) = 12.12, r(CHO) = 0.03) (Figure S20), which indicated that Sar-Sar addition was favored during the copolymerization and resulted in homo-PSar segments in P(Sar-*co*-CHO), explaining the aminolysis result.

The mechanism of the copolymerization was investigated to reveal the formation of various diad linkages. Lu(OTf)$_3$ alone was not able to catalyze homopolymerization of Sar-NCA directly (run 1 in Table S3), consistent with the result from our previous studies.[26] Whereas, it was able to catalyze the homopolymerization of CHO slowly (run 2 in Table S3). In the copolymerization of Sar-NCA with CHO, the active growing species were formed by the reaction between CHO and Lu(OTf)$_3$, illustrating the observation of PCHO oligomers in the aminolysis product. In order to determine that the copolymerization followed an AROP mechanism rather than a cationic ring-opening polymerization (CROP), a CROP inhibitor, triphenylphosphine (P(Ph)$_3$), was intentionally added.[27−29] Since P(Ph)$_3$ did not initiate a nucleophilic polymerization of NCA (run 1 in Table S4), P(Ph)$_3$ only inhibited CROP without inducing any other polymerization. After the addition of P(Ph)$_3$, the copolymerization still proceeded smoothly producing P(Sar-*co*-CHO) copolymers (run 2 in Table S4). Therefore, the copolymerization followed an anionic pathway rather than a cationic one.

A coordination AROP mechanism was proposed, as shown in Scheme 2. In initiation, epoxide rings opened to form Lu−O living species after reaction with Lu(OTf)$_3$. The reaction was

https://doi.org/10.1021/acs.macromol.5c01539
Macromolecules 2025, 58, 9450−9458

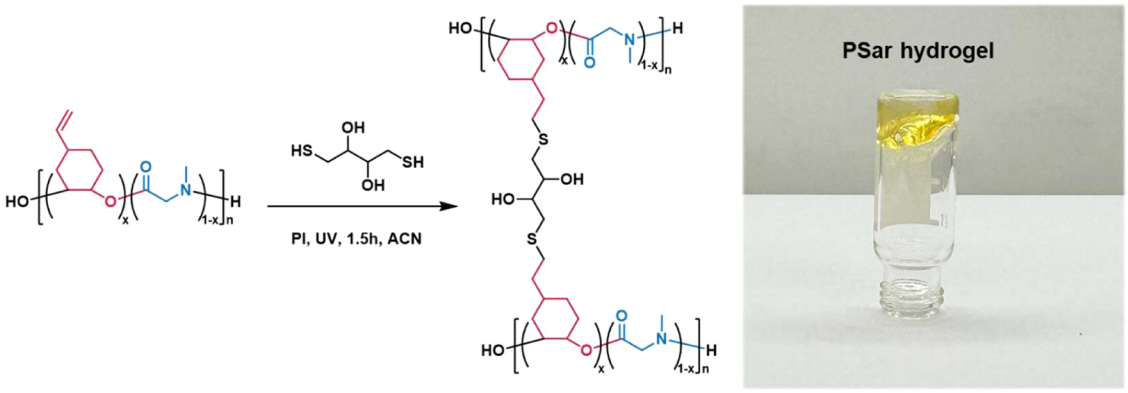

Figure 3. Preparation of PSar hydrogel via thio-ene click reaction (PI, photoinitiator, 2-hydroxy-4′-(2-hydroxyethoxy)-2-methylpropiophenone).

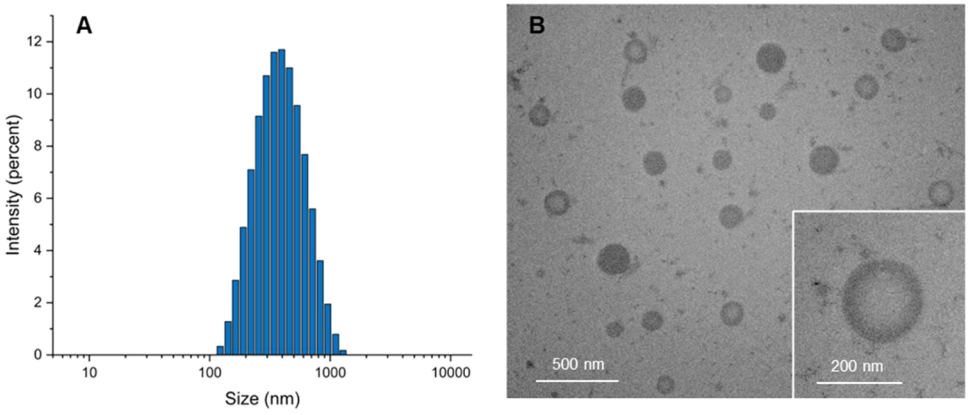

Figure 4. DLS distribution (A) and TEM images (B) of P(Sar-*co*-CHO) nanoparticles (run 12 in Table 1) in water.

investigated in detail by mixing CHO and $Lu(OTf)_3$ in equimolar amounts for ^1H NMR analysis (Figure S21). The proton signal of *O*-methine from CHO shifted from 3.11 to 3.16 ppm after coordinating $Lu(OTf)_3$. The formation of alkyl triflate and Lu−O bond after the ring cleavage of CHO was validated by the appearance of signals at 4.0−5.0 ppm (H_d, methine neighboring triflate) and 3.5−4.0 ppm (H_e, *O*-methine). The Lu−O growing center allowed the insertion of both Sar-NCA and CHO monomers, followed by ring-opening and propagation. It was in accordance with the previous report of lutetium alkoxide-mediated ROP of NCAs.[26] More specifically, Sar-NCA propagation followed a coordination and insertion mechanism and was accompanied by the release of CO_2, during which the other type of living center, the Lu-amine bond, was formed after an NCA insertion. Besides Sar-NCA, Lu-amine bond was also active to CHO insertion to generate Sar-CHO diads. Similar catalysis of rare earth triflates on the model reaction of epoxides with amines to prepare *β*-amine alcohols had been reported.[30,31] The copolymerization was terminated by water to produce copolymers with a hydroxyl group at one chain end and either an amino group from Sar-NCA or a hydroxyl group from CHO at the other end.

To verify the versatility of catalysts, we employed other rare earth triflates ($Sc(OTf)_3$ and $La(OTf)_3$) and transition-metal triflates ($Fe(OTf)_3$, $Ni(OTf)_2$, $Cu(OTf)_2$, and $Zn(OTf)_2$) to catalyze the copolymerization of Sar-NCA with CHO (Table S5). All of them except $Cu(OTf)_2$ showed good catalytic performance as Sar-NCA was completely consumed within 2 days producing P(Sar-*co*-CHO) copolymers with unimodal SEC traces (Figure S22). All of the products were composed of Sar residues and CHO units, though the CHO contents were less than that catalyzed by $Lu(OTf)_3$ under the same conditions (Table S5, run 1 in Table 1). The copolymerization was extended to other *N*-substituted glycine NCAs including *N*-ethyl glycine NCA (NEG-NCA), *N*-*n*-butyl glycine NCA (NBG-NCA), *N*-*n*-hexyl glycine NCA (NHG-NCA), and *N*-benzyl glycine NCA (NBnG-NCA). The copolymers of *N*-alkyl or *N*-aryl glycine residues and CHO units were successfully synthesized, catalyzed by $Lu(OTf)_3$ (runs 18−25 in Table 1) and characterized by NMR and SEC (Figures S23−S31). All of these compounds exhibited unimodal distributions in SEC measurements. In addition, PO and VCHO were used to copolymerize with Sar-NCA (runs 13−17 in Table 1). The corresponding random copolymers were successfully obtained by the same protocol and were confirmed by NMR and SEC analyses (Figures S32−S35).

Functionalized polypeptoids were accessible through the copolymerization of NCA with the designed epoxides. As an example, P(Sar-*co*-VCHO) (Sar% = 87 wt %, run 13 in Table 1), a degradable PSar with multiple vinyl pendant groups, was prepared by the copolymerization of Sar-NCA with VCHO initiated by $Lu(OTf)_3$. The introduction of VCHO allowed postpolymerization modification through thio-ene click reaction. A PSar gel was obtained after it reacted with dithiol reagents of D,L-dithiothreitol under a UV light of 365 nm. A solvent exchange process made it a hydrogel with a water swelling ratio of 610% (Figure 3).

Containing hydrophilic sarcosine segments and hydrophobic CHO ones, the copolymers P(Sar-*co*-CHO) (Sar% = 59 wt %,

https://doi.org/10.1021/acs.macromol.5c01539
Macromolecules 2025, 58, 9450−9458

run 12 in Table 1) self-assembled into nanoparticles in water with an average diameter of 421 nm by dynamic light scattering (DLS) (Figure 4A). The transmission electron microscopy (TEM) images revealed their spherical morphologies with diameters of ca. 200 nm (Figure 4B).

Homopolymers of PSar were not degradable by any enzyme.[1,32] On the contrary, P(Sar-*co*-CHO) was biodegradable by lipase due to the presence of ester linkages of CHO-Sar diads. The $M_{n,SEC}$ of copolymers decreased from 8.9 to 3.1 kg/mol after a 36 h incubation with porcine pancreatic lipase at 37 °C and further decreased to 2.3 kg/mol after a week (Figures 2D and S36 and Table S6). The biocompatibility of P(Sar-*co*-CHO) was assessed via a cell viability test, with CCK-8 as the indicator. After a 24 h incubation, no evident cytotoxic effects were observed in the NIH 3T3 cell lines at concentrations ranging from 1 to 500 μg/mL, indicating the noncytotoxicity of P(Sar-*co*-CHO) (Figure S37).

The thermal properties of the copolymers were investigated by DSC (Figure 5 and Table 2). P(Sar-*co*-CHO) and P(NEG-*co*-CHO) exhibited two glass-transition temperatures (T_gs) in their DSC curves. The lower one ($T_{g,1}$: P(CHO-*co*-Sar) = 25.6 °C, P(CHO-*co*-NEG) = 43.7 °C) was attributed to PCHO segments,[33] while the other ($T_{g,2}$: P(CHO-*co*-Sar) = 82.8 °C, P(CHO-*co*-NEG) = 132.3 °C) was attributed to homo-PSar or homo-PNEG segments in accord with previous reports.[22,34] The DSC curve of P(NBG-*co*-CHO) exhibited a melting temperature ($T_{m,2}$) at 182.3 °C attributed to the crystallization of homo-PNBG segments.[22] P(NHG-*co*-CHO) exhibited two melting temperatures (T_ms) in its DSC curve because of the presence of homo-PNHG segments with long alkyl side chains.[22] $T_{m,1}$ (82.8 °C) was attributed to the crystallization of the *n*-hexyl side chains while $T_{m,2}$ (141.6 °C) to the crystallization of the backbone of homo-PNHG. Compared with $T_{m,2}$ of homopolypeptoids (Table 2), $T_{m,2}$ of copolymers decreased by 45 °C (P(NBG-*co*-CHO)) and 58 °C (P(NHG-*co*-CHO)), respectively, indicating that the crystallization of polypeptoid segments was hindered by the scattering of CHO units along the backbone.

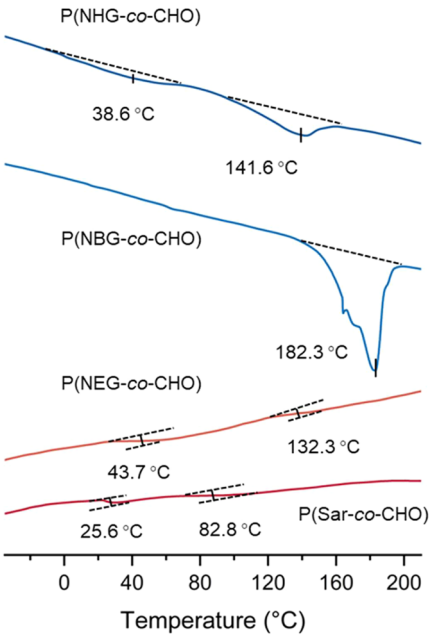

Figure 5. DSC curves (endo down) of copolymers of the second heating scan.

CONCLUSIONS

Statistical copolymers containing amide, ester, ether, and tertiary amine linkages were synthesized in one step via the copolymerizations of *N*-substituted glycine NCAs with epoxides. It facilitated greater variation in the structure and properties of polypeptoid-based materials and provided a novel insight into the copolymerization of NCA with nitrogen-free monomers. Random copolymerization of *N*-substituted glycine NCAs with epoxides was catalyzed by $Lu(OTf)_3$ or other metal triflates including $Fe(OTf)_3$, $Sc(OTf)_3$, etc. Taking the copolymerization of Sar-NCA and CHO as an example, the molar ratio of CHO to Sar in the obtained copolymers was tunable between 0.17:1 and 0.51:1, and the $M_{n,SEC}$ was designable between 2.4 and 27.0 kg/mol. The random structure of P(Sar-*co*-CHO) was confirmed by NMR, SEC, and MALDI-ToF MS. Sar-NCA tended to homopolymerize, while CHO preferred to copolymerize according to the kinetic study and the measured reactivity ratios of 12.12 and 0.03, respectively. A coordination AROP mechanism was proved, where NCA and CHO copolymerized via coordination with and insertion into the Lu−O or Lu−N bond accompanied by the release of CO_2 from NCA units. The copolymerization paradigm was successfully extended to other alkyl or aryl *N*-substituted NCAs, including NEG-NCA, NBnG-NCA, etc., and epoxides like PO and VCHO. P(Sar-*co*-VCHO) with vinyl side groups was synthesized and cross-linked to be a hydrogel after thio-ene click reaction with D,L-dithiothreitol. The nontoxic copolymers biodegradable by porcine pancreatic lipase were promising biomaterials in drug delivery.

Table 2. Glass-Transition and Melting Temperatures of the Polymers

	run	sample	[AA]:[CHO][a]	$T_{g,1}$ (°C)	$T_{g,2}$ (°C)	$T_{m,1}$ (°C)	$T_{m,2}$ (°C)
this work	1	P(Sar-*co*-CHO)	1:0.46	25.6	82.8		
	2	P(NEG-*co*-CHO)	1:0.24	43.7	132.3		
	3	P(NBG-*co*-CHO)	1:0.30				182.3
	4	P(NHG-*co*-CHO)	1:0.45			38.6	141.6
previous reports[b]	5[33]	PCHO	0:1	29.2			
	6[34]	PSar	1:0		98		
	7[22]	PNEG	1:0		96		
	8[22]	PNBG	1:0			−65	227
	9[22]	PNHG	1:0			27	200

[a]Molar ratio in polymers, AA:α-amino acid residues. [b]Samples reported by previous reports with references in superscript.

https://doi.org/10.1021/acs.macromol.5c01539
Macromolecules 2025, 58, 9450−9458

■ ASSOCIATED CONTENT

Supporting Information

The Supporting Information is available free of charge at https://pubs.acs.org/doi/10.1021/acs.macromol.5c01539.

The experimental details, characterizations on NCA monomers, and copolymers. (PDF)

■ AUTHOR INFORMATION

Corresponding Author

Jun Ling − *MOE Key Laboratory of Macromolecular Synthesis and Functionalization, Department of Polymer Science and Engineering, Zhejiang University, Hangzhou 310058, China;* orcid.org/0000-0002-0365-1381; Email: lingjun@zju.edu.cn

Authors

Keke Zhang − *MOE Key Laboratory of Macromolecular Synthesis and Functionalization, Department of Polymer Science and Engineering, Zhejiang University, Hangzhou 310058, China*

Weier Wu − *MOE Key Laboratory of Macromolecular Synthesis and Functionalization, Department of Polymer Science and Engineering, Zhejiang University, Hangzhou 310058, China*

Tianlun Shen − *MOE Key Laboratory of Macromolecular Synthesis and Functionalization, Department of Polymer Science and Engineering, Zhejiang University, Hangzhou 310058, China*

Peng Zhou − *MOE Key Laboratory of Macromolecular Synthesis and Functionalization, Department of Polymer Science and Engineering, Zhejiang University, Hangzhou 310058, China*

Tianwen Bai − *College of Biological, Chemical Sciences and Engineering, Jiaxing University, Jiaxing 314001, China; Key Laboratory of Medical Electronics and Digital Health of Zhejiang Province, Jiaxing University, Jiaxing 314001, China;* orcid.org/0000-0003-1033-9756

Complete contact information is available at: https://pubs.acs.org/10.1021/acs.macromol.5c01539

Notes

The authors declare no competing financial interest.

■ ACKNOWLEDGMENTS

This work was financially supported by the National Natural Science Foundation of China (22271252 and 22201105). The authors acknowledge Dr. Xinning Zhang from the Testing and Analysis Center of the Department of Polymer Science and Engineering at Zhejiang University for the assistance in performing TEM measurements.

■ REFERENCES

(1) Secker, C.; Brosnan, S. M.; Luxenhofer, R.; Schlaad, H. Poly(α-peptoid)s revisited: synthesis, properties, and use as biomaterial. *Macromol. Biosci.* **2015**, *15* (7), 881−891.

(2) Zhang, D.; Lahasky, S. H.; Guo, L.; Lee, C.-U.; Lavan, M. Polypeptoid materials: current status and future perspectives. *Macromolecules* **2012**, *45* (15), 5833−5841.

(3) Birke, A.; Ling, J.; Barz, M. Polysarcosine-containing copolymers: synthesis, characterization, self-assembly, and applications. *Prog. Polym. Sci.* **2018**, *81*, 163−208.

(4) Yuan, J.; Zhang, Y.; Li, Z.; Wang, Y.; Lu, H. A S-Sn Lewis pair-mediated ring-opening polymerization of α-amino acid N-carboxyanhydrides: fast kinetics, high molecular weight, and facile bioconjugation. *ACS Macro Lett.* **2018**, *7* (8), 892−897.

(5) Wang, X.; Song, Z.; Tan, Z.; Zhu, L.; Xue, T.; Lv, S.; Fu, Z.; Zheng, X.; Ren, J.; Cheng, J. Facile synthesis of helical multiblock copolypeptides: minimal side reactions with accelerated polymerization of N-carboxyanhydrides. *ACS Macro Lett.* **2019**, *8* (11), 1517−1521.

(6) Wang, S.; Lu, M.-Y.; Wan, S.-K.; Lyu, C.-Y.; Tian, Z.-Y.; Liu, K.; Lu, H. Precision synthesis of polysarcosine via controlled ring-opening polymerization of N-carboxyanhydride: fast Kinetics, ultra-high molecular weight, and mechanistic Insights. *J. Am. Chem. Soc.* **2024**, *146* (8), 5678−5692.

(7) Birke, A.; Huesmann, D.; Kelsch, A.; Weilbächer, M.; Xie, J.; Bros, M.; Bopp, T.; Becker, C.; Landfester, K.; Barz, M. Polypeptoid-block-polypeptide copolymers: synthesis, characterization, and application of amphiphilic block copolypept(o)ides in drug formulations and miniemulsion techniques. *Biomacromolecules* **2014**, *15* (2), 548−557.

(8) Bauer, T. A.; Alberg, I.; Zengerling, L. A.; Besenius, P.; Koynov, K.; Slütter, B.; Zentel, R.; Que, I.; Zhang, H.; Barz, M. Tuning the cross-linking density and cross-linker in core cross-linked polymeric micelles and its effects on the particle stability in human blood plasma and mice. *Biomacromolecules* **2023**, *24* (8), 3545−3556.

(9) Lau, K. H. A.; Sileika, T. S.; Park, S. H.; Sousa, A. M. L.; Burch, P.; Szleifer, I.; Messersmith, P. B. Molecular design of antifouling polymer brushes using sequence-specific peptoids. *Adv. Mater. Interfaces* **2015**, *2* (1), No. 1400225.

(10) Statz, A. R.; Meagher, R. J.; Barron, A. E.; Messersmith, P. B. New peptidomimetic polymers for antifouling surfaces. *J. Am. Chem. Soc.* **2005**, *127* (22), 7972−7973.

(11) Wang, J.; Zhou, P.; Shen, T.; Xu, S.; Bai, T.; Ling, J. Glycine N-thiocarboxyanhydride: a key to glycine-rich protein mimics. *ACS Macro Lett.* **2023**, *12* (11), 1466−1471.

(12) Fu, X.; Lin, X.; Wang, M.; Ding, Z.; Ma, G.; Wang, B.; Li, Y. One-step synthesis of sequence-defined polypeptide-block-polyester by Lewis pair-catalyzed chemo-selective copolymerization. *Macromolecules* **2024**, *57* (12), 5691−5701.

(13) Thompson, M. S.; Johnson, S. A.; Gonsales, S. A.; Brown, G. M.; Kristufek, S. L.; Byers, J. A. Adding polypeptides to the toolbox for redox-switchable polymerization and copolymerization catalysis. *Macromolecules* **2023**, *56* (8), 3024−3035.

(14) Zhou, P.; Shen, T.; Ling, J. Synthesis and properties of polypeptoid-containing block copolymers: a review. *J. Polym. Sci.* **2021**, *59* (23), 2946−2958.

(15) Xiong, W.; Yue, T.; Lai, H.; Lyu, C.; Ren, W.; Lu, H. Synthesis of poly(thiourethane-alt-thioester) by alternating ring-opening copolymerization of N-thiocarboxyanhydrides and episulfides. *Sci. China Chem.* **2024**, *67* (9), 3091−3097.

(16) Gu, L.; Jiang, Y.; Hu, J. Scalable spider-silk-like supertough fibers using a pseudoprotein polymer. *Adv. Mater.* **2019**, *31* (48), No. 1904311.

(17) Le Hellaye, M.; Fortin, N.; Guilloteau, J.; Soum, A.; Lecommandoux, S.; Guillaume, S. M. Biodegradable polycarbonate-b-polypeptide and polyester-b-polypeptide block copolymers: synthesis and nanoparticle formation towards biomaterials. *Biomacromolecules* **2008**, *9* (7), 1924−1933.

(18) Dorresteijn, R.; Ragg, R.; Rago, G.; Billecke, N.; Bonn, M.; Parekh, S. H.; Battagliarin, G.; Peneva, K.; Wagner, M.; Klapper, M.; Müllen, K. Biocompatible polylactide-block-polypeptide-block-polylactide nanocarrier. *Biomacromolecules* **2013**, *14* (5), 1572−1577.

(19) Zhou, P.; Dai, X.-G.; Kong, J.; Ling, J. Synthesis of well-defined poly(tetrahydrofuran)-b-poly(a-amino acid)s via cationic ring-opening polymerization (ROP) of tetrahydrofuran and nucleophilic ROP of N-thiocarboxyanhydrides. *Chin. J. Polym. Sci.* **2021**, *39* (6), 702−708.

(20) Zhou, P.; Li, Z.; Lu, Y.; Kong, J.; Ling, J. Telechelic triblock poly(α-amino acid)-poly(tetrahydrofuran)-poly(α-amino acid) copolymers: chain-end transformation, polymerization and pH-responsive hydrolysis†. *Chin. J. Chem.* **2021**, *39* (10), 2852−2856.

(21) Deng, Y.; Zou, T.; Tao, X.; Semetey, V.; Trepout, S.; Marco, S.; Ling, J.; Li, M.-H. Poly(ε-caprolactone)-block-polysarcosine by ring-opening polymerization of sarcosine N-thiocarboxyanhydride: synthesis and thermoresponsive self-assembly. *Biomacromolecules* **2015**, *16* (10), 3265−3274.
(22) Lee, C.-U.; Li, A.; Ghale, K.; Zhang, D. Crystallization and melting behaviors of cyclic and linear polypeptoids with alkyl side chains. *Macromolecules* **2013**, *46* (20), 8213−8223.
(23) Tian, Z.-Y.; Zhang, Z.; Wang, S.; Lu, H. A moisture-tolerant route to unprotected α/β-amino acid N-carboxyanhydrides and facile synthesis of hyperbranched polypeptides. *Nat. Commun.* **2021**, *12* (1), No. 5810.
(24) Wang, X.; Tong, R. Facile tandem copolymerization of O-carboxyanhydrides and epoxides to synthesize functionalized poly-(ester-b-carbonates). *J. Am. Chem. Soc.* **2022**, *144* (45), 20687−20698.
(25) Weiberth, F. J.; Yu, Y.; Subotkowski, W.; Pemberton, C. Demonstration on pilot-plant scale of the utility of 1,5,7-triazabicyclo[4.4.0]dec-5-ene (TBD) as a catalyst in the efficient amidation of an unactivated methyl ester. *Org. Process Res. Dev.* **2012**, *16* (12), 1967−1969.
(26) Peng, H.; Ling, J.; Shen, Z. Ring opening polymerization of α-amino acid N-carboxyanhydrides catalyzed by rare earth catalysts: polymerization characteristics and mechanism. *J. Polym. Sci., Part A: Polym. Chem.* **2012**, *50* (6), 1076−1085.
(27) You, L.; Ling, J. Janus polymerization. *Macromolecules* **2014**, *47* (7), 2219−2225.
(28) Diaz, C.; Tomković, T.; Goonesinghe, C.; Hatzikiriakos, S. G.; Mehrkhodavandi, P. One-pot synthesis of oxygenated block copolymers by polymerization of epoxides and lactide using cationic indium complexes. *Macromolecules* **2020**, *53* (20), 8819−8828.
(29) Qiu, H.; Shen, T.; Yang, Z.; Wu, F.; Li, X.; Tu, Y.; Ling, J. Janus polymerization: a one-shot approach towards amphiphilic multiblock poly(ester-acetal)s directly from 1,3-dioxolane with ε-caprolactone. *Chin. J. Chem.* **2022**, *40* (6), 705−712.
(30) Meguro, M.; Asao, N.; Yamamoto, Y. Ytterbium triflate and high pressure-mediated ring opening of epoxides with amines. *J. Chem. Soc., Perkin Trans. 1* **1994**, No. 18, 2597−2601.
(31) Procopio, A.; Gaspari, M.; Nardi, M.; Oliverio, M.; Rosati, O. Highly efficient and versatile chemoselective addition of amines to epoxides in water catalyzed by erbium(III) triflate. *Tetrahedron Lett.* **2008**, *49* (14), 2289−2293.
(32) Zhou, P.; Shen, T.; Chen, W.; Sun, J.; Ling, J. Biodegradable polysarcosine with inserted alanine residues: synthesis and enzymolysis. *Biomacromolecules* **2022**, *23* (4), 1757−1764.
(33) Wang, Z.; Zheng, W.; Yue, S.; Chen, K.; Ling, J.; Ni, X. Random terpolymer of carbon dioxide, butadiene and epoxides: synthesis, functionalization and degradability. *Chin. J. Chem.* **2024**, *42* (14), 1630−1636.
(34) Tao, X.; Deng, Y.; Shen, Z.; Ling, J. Controlled polymerization of N-substituted glycine N-thiocarboxyanhydrides initiated by rare earth borohydrides toward hydrophilic and hydrophobic polypeptoids. *Macromolecules* **2014**, *47* (18), 6173−6180.

https://doi.org/10.1021/acs.macromol.5c01539
Macromolecules 2025, 58, 9450−9458